

Quasicrystals—The impact of N.G. de Bruijn

Helen Au-Yang and Jacques H.H. Perk

Department of Physics, Oklahoma State University,
145 Physical Sciences, Stillwater, OK 74078-3072, USA

Abstract

In this paper we put the work of Professor N.G. de Bruijn on quasicrystals in historical context. After briefly discussing what went before, we shall review de Bruijn's work together with recent related theoretical and experimental developments. We conclude with a discussion of Yang–Baxter integrable models on Penrose tilings, for which essential use of de Bruijn's work has been made.

1 Introduction

1.1 Dedication

This article is devoted to the memory of one of the great mathematicians of the twentieth century, Prof. dr. N.G. de Bruijn. For this purpose, we shall describe here the important and unique contributions of de Bruijn to the development of the theory of quasicrystals together with their historical context.

We shall review several theoretical developments related to de Bruijn's work. We shall also briefly discuss Shechtman's experimental findings for which he was awarded the 2011 Nobel Prize in Chemistry and mention some recent technological applications that resulted from his discovery. Finally, we shall discuss some of our own results, explaining explicitly how de Bruijn's work has been used, but without going into the full mathematical details.

1.2 Pentagrid and Cut-and-project

Two of de Bruijn's papers [1, 2] give deep new insight into the nature of Penrose tilings [3, 4, 5] introduced by Penrose in 1974 as a mathematical curiosity and game. Penrose introduced two kinds of tiles, together with local matching rules forcing a tiling with a five-fold rotational symmetry axis.

Rather than constructing the tiling using local matching rules for the tiles that force aperiodicity, de Bruijn discovered two global construction methods starting with a five-dimensional lattice. The first method, a cut-and-project method, draws a two-dimensional plane and projects all lattice points in the five-dimensional lattice to that plane, that are within a certain distance from the plane as defined through a “window.” The other method introduces a “pentagrid” of five sets (grids) of equidistant parallel lines, with lines of different grids intersecting each other with angles of 36° and 72° ; the Penrose rhombus tiling follows then by dualization, choosing each rhombus according to the orientation of the two grid lines meeting at a vertex.

The pentagrid of de Bruijn is intimately related with the Conway worms mentioned already in Gardner’s 1977 article [5]. It is less directly related with the Ammann bars [6, 7]—special non-equidistant lines, which have the advantage, however, that one can draw them on the Penrose tiling itself, while they also define the tiling. Therefore, it was not immediately clear to many physicists how great de Bruijn’s contribution is. His is a simpler, complete, systematic and precise, mathematical description, allowing explicit calculations. The findings of Conway and Ammann, as reported, e.g., by [6, 7], were mostly left as observations with details not worked out. The advantage of the approach of de Bruijn is particularly clear in our work discussed in the final section 7.

Quasiperiodic structures had been studied by mathematicians and even appeared decorating medieval Islamic buildings. But because of the two constructions of de Bruijn we may feel justified to call the Penrose tiling a quasicrystal.

1.3 Nobel Prize in Chemistry

In 1982, while at the U.S. National Bureau of Standards near Washington, DC, Dan Shechtman observed a ten-fold scattering pattern from a metal alloy sample, that looked like an ordinary crystal. As this was contradicting long-held beliefs in the physics and chemistry communities, Shechtman was opposed by many colleagues—and even ridiculed by some of them—since his observations contradicted standard physics texts like Kittel’s [8]. Although initially rejected by referees, Shechtman succeeded in publishing his findings in 1984 [9, 10].

The early mathematical results on Penrose tilings and three-dimensional structures as discussed by Steinhardt et al. [11, 12, 13] helped convince many

of Shechtman's colleagues, especially since Mackay had even calculated a scattering pattern with ten-fold symmetry from a Penrose tiling [14, 15]. In the end, few continued their opposition, with the most prominent one being Nobel Prize winner Linus Pauling. More examples of quasicrystals were found in the laboratory and quasicrystals found several technical applications. For his pioneering work Shechtman received the 2011 Nobel Prize in Chemistry [16] for the discovery of quasicrystals.

In his Nobel lecture [17] Shechtman compared himself with a little pussycat trotting in front of a row of German shepherds, while quoting Psalm 23 in the original Hebrew and King James English, "Yea, though I walk through the valley of the shadow of death, I will fear no evil." He also quoted from Kittel's authoritative and widely-used textbook, "We cannot find a lattice that goes into itself under other rotations, such as by $2\pi/5$ radians or $2\pi/7$ radians. . . . We can make a crystal from molecules which individually have a five-fold rotation axis, but we should not expect the lattice to have a five-fold rotation axis." [8, p. 12]. These two passages in the Nobel lecture illustrate how hard it was for Shechtman to get his findings accepted by his colleagues. Finally, in the seventh edition of his textbook Kittel acknowledged the existence of quasicrystals [18, pp. 48, 49].

1.4 Applications of Quasicrystals

Quasicrystals exhibit very unusual properties and because of these they have found many technological applications [19, 20]. The 2011 Nobel Committee for Chemistry wrote [21]: "When trying out different blends of metal, a Swedish company managed to create steel with many surprisingly good characteristics. Analyses of its atomic structure showed that it consists of two different phases: hard steel quasicrystals embedded in a softer kind of steel. The quasicrystals function as a kind of armor." Quasicrystals are also bad conductors of heat and electricity and have non-stick surfaces.

Therefore, the number of applications of quasicrystals is ever increasing. Quasicrystals are now used in razor blades, thin needles made for eye surgery, materials for reuse of waste heat, surface coatings for frying pans (causing the pan to heat evenly), energy-saving light-emitting diodes (LEDs), heat insulation in engines (especially diesel engines), see e.g. [19, 20].

It may be noted that quasiperiodicity also can be generated in optical lattices [22], which may lead to a different kind of applications.

2 Prehistory

2.1 Islamic Art

One of the earliest forerunners of quasiperiodic tilings is manifested in the decoration of certain Islamic buildings [23, 24, 25]. Some examples are the Alhambra Palace, Spain, the Darb-i Imam Shrine, Isfahan, Iran, and a Madrasa, in Bukhara, Uzbekistan. As the Muslim faith did not allow images of life objects, artists and architects in Islamic countries were searching for a wider variety of geometrical structures to decorate their important buildings.

2.2 Dürer's *Unterweysung der Messung*

Albrecht Dürer (1471–1528) published a systematic study of tilings in his “*Unterweysung der Messung*” (1525). He concluded that regular triangles, squares and hexagons can fill the plane, but pentagons cannot by themselves do that without rhombi to fill the holes, see [26, bk. 2, 4 figs. 24].

Similarly, twelve pentagons make a dodecahedron, twenty equilateral triangles form an icosahedron (the dual of a dodecahedron). However, these objects cannot be stacked without either leaving free space *or* allowing partial overlaps.

2.3 Fibonacci sequences

Leonardo Fibonacci of Pisa ($\pm 1170 - \pm 1250$) not only advocated the use of Arabic notation of numbers over the Roman numerals, he also is the originator of the Fibonacci sequence,

$$1, 1, 2, 3, 5, 8, 13, 21, 34, 55, \dots, \quad F_{n+1} = F_n + F_{n-1}. \quad (1)$$

This describes the exponential growth of a rabbit population: Every time step each pair produces a new pair that needs one time interval to mature, before having their own offspring.

It is well-known that the Fibonacci numbers F_n can be expressed in terms of the golden ratio, which is commonly denoted by either τ or ϕ . Explicitly,

$$F_n = \frac{\tau^n - (1 - \tau)^n}{\tau - (1 - \tau)}, \quad \lim_{n \rightarrow \infty} \frac{F_{n+1}}{F_n} = \tau, \quad (2)$$

where

$$\tau = \frac{1 + \sqrt{5}}{2} = 1.61803\dots, \quad 1 - \tau = -\frac{1}{\tau} = \frac{1 - \sqrt{5}}{2} = -0.61803\dots \quad (3)$$

These are the solutions of $x^2 = x + 1$.

Much more recent is the geometric Fibonacci sequence: Assume A is a red line piece of length 1 and B a blue line piece of length τ . We can then concatenate them (link them together) using the rule,

$$F_1 = A, \quad F_2 = B, \quad F_3 = BA, \quad F_4 = BAB, \quad F_5 = BABBA, \quad (4)$$

$$F_6 = BABBABAB \dots, \quad F_{n+1} = F_n F_{n-1}. \quad (5)$$

The resulting F_∞ is quasiperiodic, i.e. a one-dimensional quasicrystal. A generalization of this sequence has been studied also by de Bruijn [27, 28].

2.4 Kronecker's Theorem

Kronecker formulated a well-known theorem that implies quasiperiodic sequences, known as Kronecker's Approximation Theorem [29]: If x is an irrational number, then the infinite sequence $\{x\}, \{2x\}, \{3x\}, \dots$, is uniformly and densely distributed within the unit interval. Here $\{nx\} \equiv nx - \lfloor nx \rfloor$ is the fractional part of nx , i.e. $0 \leq \{nx\} < 1$. Also, the formulation of the theorem given here is a more or less obvious extension of the original [29].

2.5 Harald Bohr—Almost periodic functions

Harald Bohr was a star of the Danish national soccer team, that won the silver medal in the 1908 Olympics beating France by 17-1 (the all-time Olympic record). During Bohr's 1910 PhD defense the room was filled with soccer fans. How unusual!

In his work on almost periodic functions, Bohr gave several constructions of functions that are not periodic, but almost repeat, i.e. $|f(t+T) - f(t)| < \epsilon$, for some $T(\epsilon)$ for given arbitrarily small ϵ [30]. This is a highly nontrivial generalization of Kronecker's sequence.

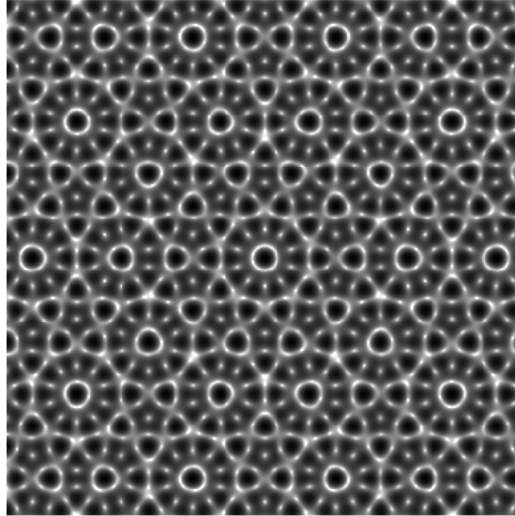


Figure 1: Fraunhofer diffraction pattern from five pinholes arranged as a pentagon. The darker the spot, the higher the intensity. Note that the center area is almost repeated at ten places near the border.

2.6 Optical example—Fraunhofer diffraction pattern

One can make the following variation of Young's double slit experiment: Illuminate five pinholes arranged as a pentagon in a screen and observe the diffraction pattern on a far-away screen. Then the local intensity on that screen is given by $I = I_0|A|^2$, with

$$A(x, y) = \sum_{j=1}^5 e^{ix \cos(\frac{2\pi}{5}j) + iy \sin(\frac{2\pi}{5}j)} \quad (6)$$

an almost-periodic analytic function of x and y .

It is very easy to plot the intensity pattern using Maple, for example:

```
f:=(x,y)->-log(abs(sum(exp(I*(x*cos(2*Pi*j/5)
+y*sin(2*Pi*j/5))),j=0..4))^2);
with(plots): d:=50; g:=400:
densityplot(f(x,y),x=-d..d,y=-d..d,grid=[g,g],
style=PATCHNOGRID,axes=NONE,scaling=CONSTRAINED);
```

The resulting pattern, see figure 1, has ten-fold rotational symmetry and thus cannot be periodic.

3 Penrose Tilings

Sir Roger Penrose, born in 1931, is a British mathematician with major contributions to general relativity and cosmology. He introduced Twistor Theory, mapping (3+1)-dimensional space-time and objects therein to a space with 2-2 signature. He also contributed to the theories of Black Holes and the Big Bang. He made some unusual observations. For example, he calculated the entropy of the universe at the Big Bang and found it to be extremely small, estimating the “Creator’s aim” to be 1 in $10^{10^{123}}$ [31, p. 344].

Penrose discovered his tilings in the early 1970s and patented them as they could be used for interesting puzzles and games. He published his invention in 1974 [3, 4] and few people knew about them before the 1977 paper of Martin Gardner [5, 6].

From the pentagon you can make two prototiles in different ways, one way being a skinny rhombus (36° - 144°) and a fat rhombus (72° - 108°). Next Penrose introduced matching rules to force the tiles into a quasiperiodic tiling: The markings on neighboring tiles have to exactly match. One can use different arrows on the edges, or colored arcs in the bodies, or matching edge deformations (to make the jigsaw effect). One can find similar matching rules for other pairs of prototiles also, like Penrose Kites and Darts [3, 4]. The result is an aperiodic tiling with the center being a five-fold rotation axis.

A well-known related tiling is the Ammann–Beenker tiling using squares and 45° - 135° rhombi. In this case the center is an eight-fold rotation axis.

It is OK to stand on a Penrose tiling like the one at Texas A & M, but when Kleenex sold toilet paper with a Penrose tiling design on it, Penrose sued the company saying that his patent was violated.

4 Nicolaas Govert de Bruijn (1918-2012)

N.G. de Bruijn started his work on quasicrystals with the one-dimensional case [27, 28] studying so-called Beatty sequences,

$$[(n + 1)\theta + \gamma] - [n\theta + \gamma], \quad [(n + 1)\theta + \gamma] - \lceil n\theta + \gamma \rceil, \quad (n \in \mathbb{Z}), \quad (7)$$

with θ and γ some constants. These sequences are in direct correspondence with generalizations of the Fibonacci lattice and also play a role in higher-dimensional tilings of Penrose type. They are differences of two sequences of the type discussed in the subsection on Kronecker's theorem.

Next, de Bruijn went to the two-dimensional Penrose case introducing the pentagrid method [1, 2], which he later generalized to the multigrid method [32]. The multigrid or n -grid is a collection of n sets of equidistant parallel lines, with lines of different sets making angles that are multiples of π/n . The tiling then is a dualization of the multigrid, assigning to each intersection of lines a rhombus with all sides perpendicular to one of the intersecting lines. The sides of all rhombi are of equal length.

More generally, de Bruijn constructed also higher-dimensional versions building quasicrystals of parallelepipeds [32], thus completing the proof that the dual of a multigrid is a tiling.

It should be noted that Gardner, in his 1977 Scientific American article [5], had already discussed the "Conway worms" discovered by Conway. In the rhombus version of the Penrose tiling, a Conway worm is a band that passes through opposite sides of a sequence of rhombi of the tiling. There are five sets of nonintersecting worms that correspond one-to-one to the pentagrid of de Bruijn.

We should also note Ammann's observation that the worms could be replaced by a quasigrid of five sets of parallel lines that are not equidistant, but their interdistances rather form a Fibonacci pattern. This is now called the Ammann quasigrid made up of five grids of Ammann bars [6, 7]. The connection with the pentagrid of de Bruijn was explicitly worked out and proved by de Bruijn himself in [33]. However, the topological deformations needed for the proof are such that one would not want to treat the two five-grid pictures as interchangeable in actual more-involved calculations on Penrose tilings like the one discussed in section 7.

The Fourier transforms of the tilings were treated by de Bruijn in [34, 35], with earlier results for the regular Penrose tiling worked out numerically by Mackay [14, 15]. For the infinite tiling this is an infinite sum of Dirac delta functions, corresponding to what physicists call the Bragg diffraction peaks.

In [36] de Bruijn made the observation that for a given infinite Penrose tiling one can find for any number $\varepsilon > 0$ two vertices so that all other infinite Penrose tilings with the same two vertices have all but a fraction ε of their vertices in common with the original tiling.

In [37] de Bruijn made a study of the inflation-deflation rules of the

Penrose tilings providing details left out by Gardner [5].

In several of the aforementioned papers de Bruijn also addressed the Cut-and-Project Method. The simplest example is the one-dimensional Fibonacci lattice seen above. It derives from the two-dimensional square lattice by cutting a narrow band out of the lattice and projecting all lattice points within the band. More precisely, choose a direction with slope given by the golden ratio and choose a properly sized window perpendicular to that direction. Then project all lattice points within the window to the sloped line. This generalizes to n and m dimensions (5 and 3 for Penrose tilings).

5 Paul Steinhardt “to the rescue”

While Shechtman was fighting referees and particularly Linus Pauling, he got a big boost from the work of Steinhardt and coworkers.

Paul Steinhardt is a cosmologist, originally at the University of Pennsylvania, but now at Princeton. He wrote many papers on such topics as Inflationary Cosmology and Cyclic Cosmology.

Up to 1984 quasiperiodic tilings was mainly a topic for mathematicians. Together with Levine, Socolar and others he introduced the works of Penrose, de Bruijn, Mackay, and later Gummelt, to the physics community, while extending these works in various directions [38, 39, 40].

Many quasicrystals have been synthesized. The obvious question was, “Do quasicrystals occur in nature?” This has been answered in the affirmative as a first natural quasicrystal has been discovered in a museum in Florence, Italy. It came from the Khatyrka River in Kamchatka, Russia [41, 42, 43].

6 Alternative approaches

6.1 Periodic approximants

Tsunetsugu et al. designed a modification of the multigrid approach of de Bruijn that produces a converging sequence of periodic approximants to the Penrose tiling [44, Appendix]. This could be extremely useful for numerical calculations on the Penrose tiling, as one can often produce very accurate numerical results for a number of approximants that may then extrapolate very well.

6.2 Inflation rules

One favorite way to create large tilings is by the repeated application of certain inflation rules [45]: Blow up all tiles and substitute each of them by a collection of the original tiles following very precise rules. The Tilings Encyclopedia [46] gives more than 180 examples.

6.3 Overlapping unit cells

Petra Gummelt designed a special decagon decorated with red and blue patches in a particular way [47] that can partially overlap with a copy in a few ways. Two neighboring decagons must overlap red-on-red and blue-on-blue. There are two types of possibilities A or B. The result is a representation of a Penrose tiling in a way that may explain how they arise from chemical interactions. “Gummelt’s Decagon as Overlapping (Quasi) Unit Cell” has, therefore, caused much interest.

Further aspects of the decagon approach were discussed in [48, 49]. This is followed by a number of studies that discuss clusters of different types of atoms and the related chemistry filling the decagon in with atoms, thus explaining how it comes about [50, 51, 52, 53]. Even comparisons with experiments are made in some of these papers [50, 54]. Other papers discuss the partial relaxation of the matching rules implied by the Gummelt decagon, so that one can construct random tilings [55, 56, 57].

Overlapping three-dimensional versions have been constructed since, see [58, 59] for a decagonal example. Using de Bruijn’s five-dimensional lattice projected down to three dimensions, rather than two for the Penrose tiling, we constructed a quasicrystal, periodic in one direction and quasiperiodic in the other two. It is made up of overlapping polytopes with 22 external vertices and 4 internal ones. But the polytopes in that model do not yet have a Gummelt-type decoration enforcing matching rules.

The 1985 paper of Shechtman and Blech [10] used non-overlapping icosahedra. This gave a description of the structure, but no complete understanding how it could come about.

7 Pentagrid Ising Model and Other Integrable Models

7.1 Planar Ising model

One area of physics, for which the de Bruijn pentagrid construction has been applied, is integrable models of statistical mechanics on quasicrystals. As an example we shall discuss those aspects of our work on the (zero-field) pentagrid Ising model [60] that relate to de Bruijn's work. Ising models on Penrose tilings belong to the class of planar Ising models. It is well-known that such Ising models in zero magnetic field can be solved in principle using Pfaffians or fermion methods [61, 62], though in practice it can become very cumbersome. We shall see that the pentagrid allows introducing an extra integrability structure facilitating detailed calculations.

A planar Ising model is defined on a planar graph, with spin variables $\sigma_j = \pm 1$ on each vertex j and interaction energy $-J_{j,j'}\sigma_j\sigma_{j'}$ associated with each edge $\langle j, j' \rangle$. In addition, each spin σ_j interacts with the magnetic field, B in suitable units, so that the total interaction energy becomes

$$\mathcal{H} = - \sum_{\langle j, j' \rangle} J_{j, j'} \sigma_j \sigma_{j'} - B \sum_j \sigma_j, \quad (8)$$

with the first sum over all edges $\langle j, j' \rangle$ of the graph and the second sum over all \mathcal{N} vertices (sites) j .

In equilibrium statistical mechanics one introduces the Boltzmann-Gibbs probability distribution

$$\rho(\{\sigma\}) = \frac{e^{-\beta\mathcal{H}}}{Z}, \quad Z = \sum_{\{\sigma\}} e^{-\beta\mathcal{H}}, \quad \beta = \frac{1}{k_B T}, \quad (9)$$

where $\{\sigma\}$ stands for all \mathcal{N} values $\sigma_j = \pm 1$, ($j = 1 \dots \mathcal{N}$), Z denotes the partition function (Zustandssumme in German) providing the normalization of ρ , while T is the absolute temperature and k_B Boltzmann's constant.

Some physical quantities of particular interest are the free energy per site

$$f = -\frac{1}{\beta\mathcal{N}} \ln \sum_{\{\sigma\}} \exp \left(\beta \sum_{\langle j, j' \rangle} J_{j, j'} \sigma_j \sigma_{j'} \right) = -\frac{1}{\beta\mathcal{N}} \ln Z \quad (10)$$

and the pair correlation of spins on sites k and l ,

$$\langle \sigma_k \sigma_l \rangle = \frac{\sum_{\{\sigma\}} \sigma_k \sigma_l \exp\left(\beta \sum_{\langle j, j' \rangle} J_{j, j'} \sigma_j \sigma_{j'}\right)}{\sum_{\{\sigma\}} \exp\left(\beta \sum_{\langle j, j' \rangle} J_{j, j'} \sigma_j \sigma_{j'}\right)} = \sum_{\{\sigma\}} \rho(\{\sigma\}) \sigma_k \sigma_l, \quad (11)$$

both in zero magnetic field, $B = 0$. In most physical applications one is interested in very large systems ($\mathcal{N} \sim 10^{23}$), so that one may just as well consider the thermodynamic limit $\mathcal{N} \rightarrow \infty$. For the quasiperiodic case of a ferromagnetic ($J_{j, j'} > 0$) Ising model on a Penrose tiling, the bulk properties are uniquely determined in this limit, irrespective of what happens at the boundaries. Another physical quantity is the single spin correlation $\langle \sigma_{\mathbf{r}} \rangle$ being evaluated in infinitesimal positive magnetic field (if all $J_{j, j'} \geq 0$), i.e.

$$\langle \sigma_k \rangle = \lim_{B \downarrow 0} \lim_{\mathcal{N} \rightarrow \infty} \frac{\sum_{\{\sigma\}} \sigma_k \exp\left(\beta \sum_{\langle j, j' \rangle} J_{j, j'} \sigma_j \sigma_{j'} + \beta B \sum_j \sigma_j\right)}{\sum_{\{\sigma\}} \exp\left(\beta \sum_{\langle j, j' \rangle} J_{j, j'} \sigma_j \sigma_{j'} + \beta B \sum_j \sigma_j\right)}. \quad (12)$$

This is positive (nonzero) for temperatures below the critical temperature, $T < T_c$. The order of limits is important [64], as in the other order we have $B = 0$ for finite \mathcal{N} , in which case the symmetry $\sigma_j \rightarrow -\sigma_j$ for all j negates $\langle \sigma_k \rangle$ implying $\langle \sigma_k \rangle \equiv 0$.

7.2 Star-triangle (Yang–Baxter) equation

For a subclass of Ising models more can be solved using an underlying Yang–Baxter equation [63], which becomes a star-triangle relation in this case, namely,

$$\begin{aligned} & \sum_{\sigma_4 = \pm 1} \exp\left(\bar{K}(u, v) \sigma_1 \sigma_4 + K(u, w) \sigma_2 \sigma_4 + \bar{K}(v, w) \sigma_3 \sigma_4\right) \\ &= R(u, v, w) \exp\left(K(v, w) \sigma_1 \sigma_2 + \bar{K}(u, w) \sigma_1 \sigma_3 + K(u, v) \sigma_2 \sigma_3\right), \end{aligned} \quad (13)$$

with $K_{j, j'} \equiv \beta J_{j, j'} = K(u, v)$ or $\bar{K}(u, v)$, depending on the orientation of the edge $\langle j, j' \rangle$ with respect to two oriented lines crossing the edge, while these

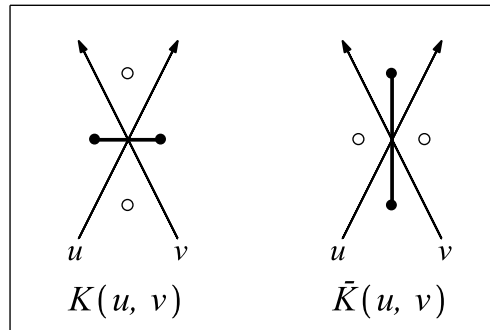
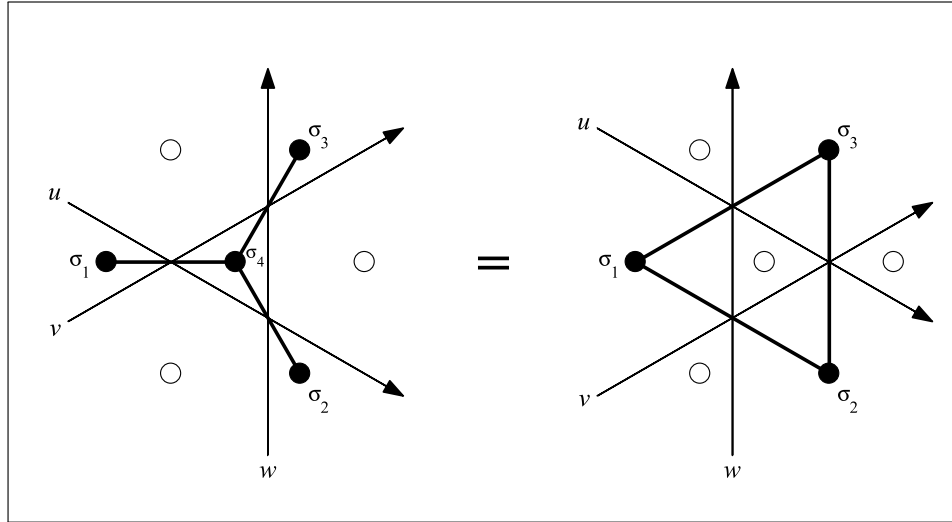


Figure 2: The star-triangle (Yang–Baxter) equation for the Ising model represented as a picture. Solid circles represent Ising spins coupled by fat lines. Open circles represent spin sites of the dual Ising model. The thin oriented lines carry the rapidity variables. The bottom picture shows the two assignments of βJ by either function $K(u, v)$ or $\bar{K}(u, v)$.

lines carry “rapidity” variables u and v , see also figure 2. Also, $R(u, v, w)$ is a factor independent of the values of σ_1 , σ_2 and σ_3 .

Equation (13), illustrated by figure 2, expresses the fact that for an Ising model so parametrized the partition function Z does not change, if any given rapidity line passes through the intersection of two other rapidity lines. Therefore, such models are called Z -invariant by Baxter [65]. Many other solutions of Yang–Baxter equations exist that are not Ising-like. For example, Baxter treats the Z -invariant eight-vertex model in the same paper [65], a model for which the Yang–Baxter equation is still pictured by figure 2, provided one couples each pair of spins connected by a fat line with the two dual spins on both sides of that line. See, e.g., [63] for various appearances of the Yang–Baxter equation.

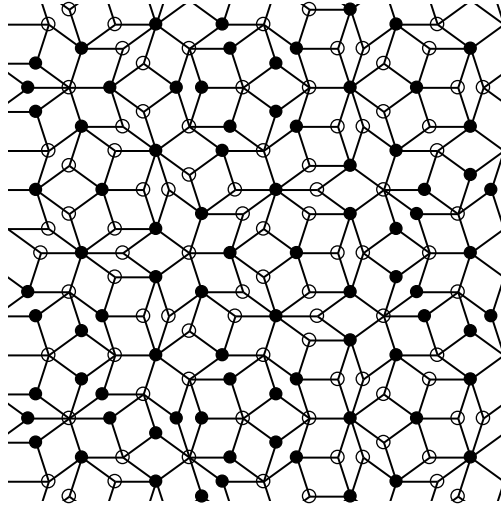


Figure 3: Part of a regular Penrose tiling of fat and skinny rhombi. The graph is bipartite, so that the vertices can be colored alternately black and white, dividing the tiling into two (quasi-)sublattices.

Korepin [66, 67, 68, 69] pioneered the eight-vertex model on a Penrose tiling. Now the rapidity variables, the free parameters in the Yang–Baxter equation, live on the grid lines of de Bruijn’s pentagrid. The model has four-spin interactions for each quadruple of vertices belonging to a rhombus of the tiling, see figure 3. This allowed Korepin to calculate the free energy per site of the model on an infinite Penrose tiling following Baxter [65, 70] and

also to apply Baxter’s “unwieldy” multiple integral formula [65] for the pair correlation in the special case that there is only two-spin interactions across all diagonals of the rhombi. This special case factorizes into two independent pentagrid Ising models.

7.3 The pentagrid Ising model

If we divide the vertices of a Penrose rhombus tiling into two sublattices as shown in figure 3, we can put an Ising model on one sublattice with Ising interactions along the diagonals of the rhombi. The other sublattice is the dual lattice of the first one, on which one can put an Ising model at the dual temperature. We have called this model, shown in figure 4, the pentagrid Ising model [60]. This last paper consists of three parts, namely,

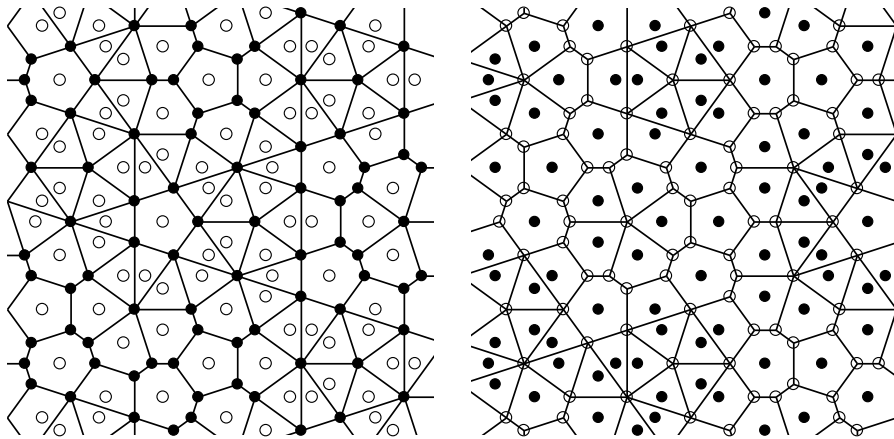


Figure 4: On the left: The pentagrid Ising model with spins on the black lattice, interacting along diagonals of the rhombi. On the right: The dual pentagrid Ising model built similarly with spins on the white lattice.

- an algebraic recursion scheme to systematically calculate results of pair correlations as functions of the rapidities on pentagrid lines “passing between” the pairs of spins, without doing Baxter’s integrals over an ever-increasing number of variables,
- a new method to determine the joint probability of two distant local

environments in the pentagrid, to connect those pair correlations with actual positions of spins,

- the explicit numerical calculation of the Fourier transform (q -dependent susceptibility or structure function) of the pentagrid-Ising-model pair correlation.

We shall next briefly describe these three items, as they relate to de Bruijn’s pentagrid construction, without going into the full details of [60].

In order to define the integrable pentagrid Ising model we start with a regular pentagrid à la de Bruijn [1, 2]—five grids of equidistant parallel lines making angles of multiples of $\pi/5$ with one another and shifted such that no three lines meet in a common intersection, see figure 5. These lines, carrying the rapidity variables, correspond to curved lines in the Penrose tiling, with each line passing through opposite sides of a sequence of rhombi in figure 3, thus identifying a grid line of the pentagrid with a “Conway worm” [5]—band of rhombi with each rhombus connected to two other ones at opposite edges.

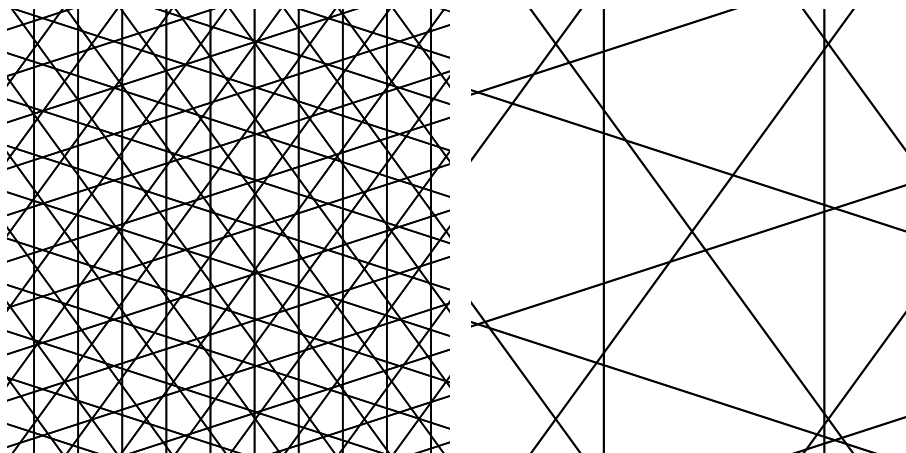


Figure 5: On the left: Part of the pentagrid. No three lines pass through a common point, even though pairs of intersections may approach arbitrarily close. On the right: The central “parallelogram” from lines of two grids with one of 24 topologically different configurations of lines from the other three grids inside. Note that multiple intersections indeed do not take place.

Grid lines can only intersect with angles of $\pi/5$ or $2\pi/5$. Following de Bruijn [1, 2], to each such intersection we assign a skinny or fat rhombus,

respectively with their sides perpendicular to the grid lines, as is shown in figure 6.

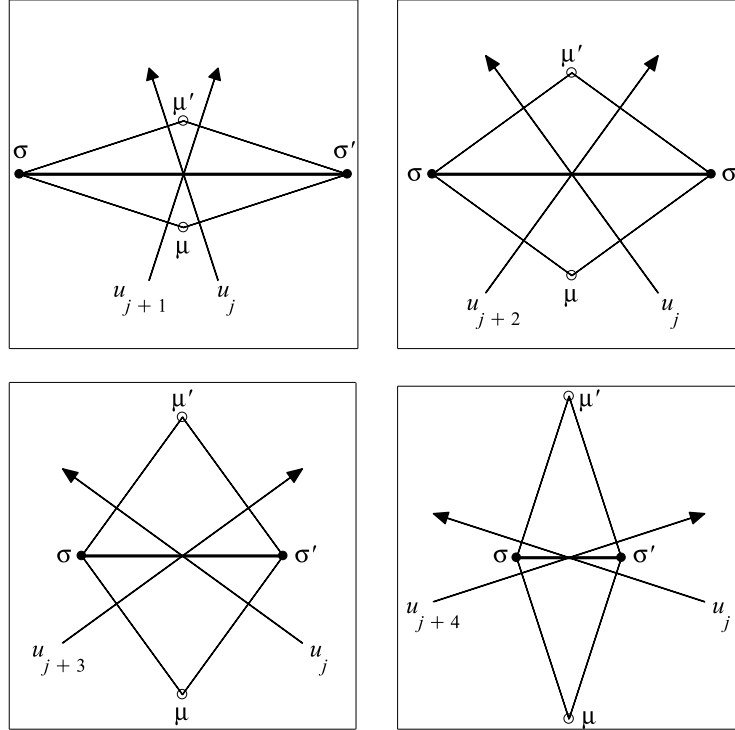


Figure 6: The four different ways to assign a rhombus to a given intersection of the pentagrid, with four different-size diagonals connecting the black vertices.

7.4 Choice of Ising interactions

We want to choose the parameters of the interactions such that the star-triangle equations hold, that the model has a five-fold symmetry axis, and that the interactions are weaker if the separation of spins is larger.

The star-triangle equation imposes a parametrization in terms of elliptic functions of modulus $0 \leq k \leq 1$, $k' = \sqrt{1 - k^2}$. This k relates to the temperature, with $k = 1$ being the critical case. For the two choices for

$\beta J = K(u, v)$ or $\bar{K}(u, v)$ in figure 2 we must choose, in the low-temperature case with $k \leq 1$ a temperature-like variable,

$$\sinh(2K(u, v)) = \text{sc}(u - v, k') = k^{-1} \text{cs}(K(k') - u + v, k'), \quad (14)$$

$$\sinh(2\bar{K}(u, v)) = k^{-1} \text{cs}(u - v, k') = \text{sc}(K(k') - u + v, k'), \quad (15)$$

with $K(k')$ the complete elliptic integral of the first kind of modulus k' and $\text{sc} = \text{sn}/\text{cn}$ and $\text{cs} = 1/\text{sc}$ Jacobi elliptic functions. In the high-temperature case, with $k^{-1} \geq 1$ temperature-like, we choose

$$\sinh(2K(u, v)) = k \text{sc}(u - v, k') = \text{cs}(K(k') - u + v, k'), \quad (16)$$

$$\sinh(2\bar{K}(u, v)) = \text{cs}(u - v, k') = k \text{sc}(K(k') - u + v, k'). \quad (17)$$

Next we must choose the rapidities, such that the model's interaction strengths are rotational invariant, only depending on the separations of spins. This is easily achieved noting that (14) through (17) only depend on k and the difference of rapidities $u - v$. Each of the five grids of the pentagrid can be oriented in two directions. Let for the j th oriented grid, grid_j , the arrow of each grid line point in the direction defined by angle

$$\phi_j = \angle \text{grid}_j = \phi_0 - j\pi/5, \quad \text{and let } u_j = jK(k')/5, \quad (18)$$

with j defined modulo 10. It is clear that then $\text{grid}_{j\pm 5}$ is the same grid as grid_j , but with the arrows reversed, and $u_{j\pm 5} = u_j \pm K(k')$. This condition for the change of rapidity with arrow reversion originates from [71, page 50].

The four pictures in figure 6 represent $\beta J = K(u_{j+l}, u_j)$, for $l = 1, \dots, 4$, see also figure 2. Inverting the arrow of the u_j -rapidity, replacing u_j by u_{j+5} , we obtain $\beta J = \bar{K}(u_{j+5}, u_{j+l})$, which is the same, as can be seen comparing (14) and (15), or (16) and (17), for the below or above critical temperature cases. We conclude that $\sinh(2\beta J) = \text{sc}(lK(k'), k')$, or $k \text{sc}(lK(k'), k')$ for $l = 1, \dots, 4$, the extra factor k being needed above the critical temperature. Indeed, the longer the diagonal the weaker the interaction. We note that Choy [72] made essentially the same choice of Ising interactions, specializing the Penrose eight-vertex model and the free energy results of Korepin [66, 67], but he did not derive new results for correlation functions.

7.5 Pair correlations in terms of rapidities

The traditional way to calculate pair correlation function (11) in infinite planar Ising models is using either fermion (Clifford algebra) methods or

equivalent dimer problems [61, 62]. If the spin pair lies on an axis of reflection symmetry, this leads to Toeplitz determinants, but in general the computation can become quite cumbersome.

In many cases, the work can be greatly reduced with the help of quadratic identities for the pair correlations [73], enabling one to exactly calculate all pair correlation functions one-by-one recursively. These identities can be seen as a general Wick theorem for fermions or as a compound Pfaffian theorem [74]. Further simplification occurs if the model has an underlying Z -invariance [65, 71]. Since the pentagrid Ising model is defined through rapidities on the pentagrid, this applies [60] also for this case.

Let us explain this in more detail. Consider a pair of spins in the bulk of a very large but finite Z -invariant Ising model. All edges of the model correspond to intersections of pairs of rapidity lines. Bend, if necessary, the rapidity lines such that there are no further intersections as they go off to infinity. Then the edges of the Ising model are in one-to-one correspondence with the intersections of the rapidity lines. We can now play Baxter's game of moving rapidity lines to or from infinity, making changes on the boundary of the Ising model that cause perimeter-to-area effects in the free energy per site that vanish in the infinite system limit.¹

We can bend a rapidity line that goes through the bulk of the model, but does not pass between the pair of spins considered, such that it now intersects outside the model boundary with a sequence of other rapidity lines. Then, applying the star-triangle equation of figure 2 several times, we can move that rapidity line to the boundary. Similarly, we can introduce a new rapidity line at the boundary and move it to go near the spin pair considered. However, we cannot move rapidity lines that cross between spins in and out from there; we can only change their ordering.

Consequently, the pair correlation cannot depend on rapidity variables of rapidity lines that do not cross between the spin pair. It does depend on the elliptic modulus and the set of rapidity variables on the even number, say $2n$, of lines that do cross between the spins. With Baxter [65] we can now introduce universal functions $g_{2n}(\{u_1, \dots, u_{2n}\}, k)$, for $n = 0, 1, 2, \dots$, and similarly g_{2n}^* for the dual Ising model (with spins on the open circles rather

¹The pair correlation has high- and low-temperature expansions that are uniformly convergent within radii of convergence (expected to correspond to modulus $k = 1$), with more and more coefficients taking their limiting values as the boundary moves away from the two spins with increasing system size.

than the solid circles in figures 3 and 4). More explicitly,

$$\langle \sigma_i \sigma_j \rangle = g_{2n}(\{u_1, \dots, u_{2n}\}, k), \quad \text{or} \quad g(u_1, \dots, u_{2n}) \quad \text{for short}, \quad (19)$$

where u_1, \dots, u_{2n} is any ordering of the rapidities of the rapidity lines passing between sites i and j in the same direction. As said below (18), changing the direction of rapidity line k results in the replacement $u_k \rightarrow u_k \pm K(k')$. Obviously, $g_0 \equiv g_0^* \equiv 1$, as $\sigma_i^2 = (\pm 1)^2 = 1$.

With the notation of (19) the quadratic identities of [73] become

$$\begin{aligned} & \text{sc}(u_2 - u_1, k') \text{sc}(u_4 - u_3, k') \\ & \quad \times \{g(u_1, u_2, u_3, u_4, \dots)g(\dots) - g(u_1, u_2, \dots)g(u_3, u_4, \dots)\} \\ & + \{g^*(u_1, u_3, \dots)g^*(u_2, u_4, \dots) - g^*(u_1, u_4, \dots)g^*(u_2, u_3, \dots)\} = 0, \\ \\ & k^2 \text{sc}(u_2 - u_1, k') \text{sc}(u_4 - u_3, k') \\ & \quad \times \{g^*(u_1, u_2, u_3, u_4, \dots)g^*(\dots) - g^*(u_1, u_2, \dots)g^*(u_3, u_4, \dots)\} \\ & + \{g(u_1, u_3, \dots)g(u_2, u_4, \dots) - g(u_1, u_4, \dots)g(u_2, u_3, \dots)\} = 0, \end{aligned} \quad (20)$$

where all “ \dots ” stand for the same (but arbitrary) even set of u_j 's, see [75, 76]. From these one can systematically derive all g_{2n} and g_{2n}^* iteratively with increasing n , provided one knows these for the two cases with all or all but one of the u_j 's equal. For the pentagrid Ising model paper [60], these special cases were evaluated by iteration from determinant formulae in [75]. Now there is a more efficient way, discovered by Witte [77] and described in detail in [78, section 3].

Finally, the single-spin correlation (12) cannot depend on any rapidity variable. Therefore [65, 70],

$$\langle \sigma_i \rangle \equiv k'^{1/4} \quad \text{for all sites } i, \quad (21)$$

below criticality, and zero above. Because of this property, it is also called order parameter or spontaneous magnetization per site.

7.6 Integer quintuples, indices, and probabilities

So far we have not used the more technical part of de Bruijn's work on Penrose tilings. If one only wants to know the free energy per site of the pentagrid Ising model in the thermodynamic limit, one just needs the idea

of the pentagrid construction and the ratio of the numbers of fat and skinny rhombi in an infinite Penrose tiling. Everything else needed is supplied by Baxter [65]. The order parameter (21) is even a freebie in Baxter's approach.

However, once we want to know more about the magnetic structure of the model as is contained in the pair correlation, we need to know the precise position of spins in relation to the pentagrid. We also need a prescription to determine if a spin is in the black (even) or in the white (odd) sublattice of figure 3. Finally, we need the joint probability of the occurrence of two local configurations that are an arbitrary distance apart. For all these we need many technical details of [1, 2, 27], as is explained more fully in [60]. Here we shall outline the ideas, especially the use of sections 4 and 5 of [1].

First of all, de Bruijn introduces the five grids G_j , with the lines of the j th grid labeled by integers k_j , i.e.,

$$G_j = \{z \in \mathbb{C} | \text{Re}(z\zeta^{-j}) + \gamma_j = k_j, k_j \in \mathbb{Z}\}, \quad j = 0, \dots, 4. \quad (22)$$

where

$$\zeta = e^{2i\pi/5}, \quad \zeta + \zeta^{-1} = 2 \cos(2\pi/5) = \tau^{-1} = \frac{1}{2}(\sqrt{5} - 1), \quad (23)$$

in which τ is the golden ratio and the γ_j are five real numbers satisfying $\sum_{j=0}^4 \gamma_j = 0$. Grid G_j corresponds to grid_{2j} with $\phi_0 = 0$ in (18). One can easily choose the γ_j such that the pentagrid is regular, nowhere three or more grid lines having a common intersection.

The vertices of the Penrose tiling correspond to the meshes, or faces, of the pentagrid. These meshes are determined by a quintuple of integers, the integer vector $\vec{K}(z) = (K_0(z), \dots, K_4(z))$ —defined the same for each point $z \in \mathbb{C}$ of the mesh—using

$$K_j(z) = \lceil \text{Re}(z\zeta^{-j}) + \gamma_j \rceil, \quad (24)$$

with $\lceil x \rceil$ denoting the ceil or roof of x , i.e. the smallest integer $\geq x$. It is easily seen from (22) and (24) that whenever z moves across a line of the j th grid, $K_j(z)$ changes by 1 and that the meshes are in one-to-one correspondence with these integer vectors.

A particular useful property discovered by de Bruijn [1] and exploited in [60] is that the sum of the five integers satisfies

$$\text{Index}(z) \equiv \sum_{j=0}^4 K_j(z) = 1, 2, 3, \text{ or } 4, \quad (25)$$

by which we can distinguish if the corresponding vertex of the Penrose tiling,

$$f(z) = \sum_{j=0}^4 K_j(z)\zeta^j, \quad (26)$$

belongs to the even (Index = 2, 4) or the odd (Index = 1, 3) sublattice of figure 3, i.e., if it belongs to the Ising or the dual Ising model in figure 4.

One way to systematically account for all vertices of the infinite Penrose tiling is to divide the pentagrid space into parallelograms by grids G_0 and G_1 . Let $P(k_0, k_1)$ be the parallelogram bounded by lines $k_0 - 1$ and k_0 of G_0 and $k_1 - 1$ and k_1 of G_1 , defined in (22). The lines of the other three grids can pass through $P(k_0, k_1)$ in 24 topologically distinct configurations, with one example shown in figure 5 and all 24 cases in [60, fig. 6]. It is easily verified that this way $P(k_0, k_1)$ is split into 6 to 12 meshes (or faces) depending on the configuration.

It is convenient to single out one mesh of $P(k_0, k_1)$ that corresponds to a vertex of the even sublattice of the Penrose tiling. For this purpose we introduced the reference integer vector (k_0, \dots, k_4) , which is related to the extreme corner z_c of $P(k_0, k_1)$ where the lines labeled by k_0 and k_1 cross. Thus we chose

$$\begin{aligned} k_0 &= K_0(z_c), & k_1 &= K_1(z_c), \\ k_2 &= \lceil \alpha \rceil - k_0 = K_2(z_c), & k_4 &= \lceil \beta \rceil - k_1 = K_3(z_c), \end{aligned} \quad (27)$$

with $\lceil x \rceil$ the roof or ceiling of x and

$$\alpha \equiv \tau^{-1}(k_1 - \gamma_1) + \gamma_0 + \gamma_2, \quad \beta \equiv \tau^{-1}(k_0 - \gamma_0) + \gamma_1 + \gamma_4, \quad (28)$$

which can be easily derived. However, for the last component of the reference integer vector we chose

$$k_3 = 2 - \lceil \alpha \rceil - \lceil \beta \rceil = -\lfloor \alpha \rfloor - \lfloor \beta \rfloor \neq K_3(z_c) = \lceil -\alpha - \beta \rceil, \quad (29)$$

with $\lfloor x \rfloor$ denoting the ‘‘floor of x ’’, i.e. the largest integer $\leq x$. The index of the reference integer vector is $\sum_j k_j = 2$, so that (k_0, \dots, k_4) indeed labels a mesh corresponding to the even sublattice. On the other hand,

$$K_3(z_c) = \begin{cases} k_3 - 1 & \text{for } \{\alpha\} + \{\beta\} \geq 1, \\ k_3 & \text{for } \{\alpha\} + \{\beta\} < 1, \end{cases} \quad (30)$$

using the notation $\{x\} \equiv x - [x]$ for the fractional part of x .

This shows that only for $\{\alpha\} + \{\beta\} < 1$ the mesh adjacent to the extreme corner z_c belongs to the even sublattice, its integer vector $\vec{K}(z_c)$ being the reference integer vector of $P(k_0, k_1)$. This is not so if $\{\alpha\} + \{\beta\} \geq 1$, in which case $\vec{K}(z_c)$ corresponds to an odd vertex. That in one of the 24 configurations the reference integer vector lies outside $P(k_0, k_1)$ is not a problem, as now $\{\alpha\} + \{\beta\} \geq 1$ determines the nature (odd/even) of the mesh adjacent to z_c and the corresponding vertex of the Penrose tiling.

The introduction of the variables α and β in (28) is one of the main tricks in [60]. The values of $\{\alpha\}$ and $\{\beta\}$ determine in which of the 24 configurations $P(k_0, k_1)$ is. It is straightforward to denote in the unit square of plotting $\{\alpha\}$ versus $\{\beta\}$ the area corresponding to each configuration. It is also clear from (28) and Kronecker's theorem of subsection 2.4, that the points $(\{\alpha\}, \{\beta\})$ are uniformly and densely distributed as k_0 and k_1 run through all integers. The probability of a configuration becomes simply the magnitude of an area in the unit square!

For the determination to a pair correlation with spins having positions corresponding to meshes in $P(k_0, k_1)$ and $P(k_0 + \Delta k_0, k_1 + \Delta k_1)$, we can determine the shift $(\Delta\alpha, \Delta\beta)$ from (28). It is easy to find the joint probability of having given configurations of the two parallelograms, as k_0 and k_1 run through all integers, but with Δk_0 and Δk_1 kept fixed. It is now expressed through the areas of overlap of areas in the above unit square and another square where the areas are shifted cyclically by $(\Delta\alpha, \Delta\beta)$. This gives 24×24 probabilities.

However, for the regular Penrose tiling we do not have to consider all $576 = 24^2$ possibilities separately, as we can combine many cases together. The way [60] is set up, for the odd quasi-lattice we end up with 8^2 possibilities and for the even quasi-lattice 16^2 . We could even prove that the $\chi(\mathbf{q})$, defined in the next subsection, is the same for both quasi-lattices. This reduction does not occur for nonregular Penrose tilings [59], even though we may expect these to lead to the same values of $\chi(\mathbf{q})$.

7.7 Wavevector-dependent susceptibility

A quantity of particular interest in physics is the wavevector-dependent susceptibility $\chi(q_x, q_y)$, which is the Fourier transform of the connected pair

correlation. More precisely,

$$\chi(\mathbf{q}) = \beta \lim_{\mathcal{L} \rightarrow \infty} \frac{1}{\mathcal{L}} \sum_{\mathbf{r}} \sum_{\mathbf{r}'} e^{i\mathbf{q} \cdot (\mathbf{r}' - \mathbf{r})} [\langle \sigma_{\mathbf{r}} \sigma_{\mathbf{r}'} \rangle - \langle \sigma_{\mathbf{r}} \rangle \langle \sigma_{\mathbf{r}'} \rangle], \quad (31)$$

where $\mathbf{q} = (q_x, q_y)$ while \mathbf{r} and \mathbf{r}' are the physical positions of the vertices on which the spin variables live. The sums are done over all spin positions in finite patches \mathcal{L} of the Penrose tiling and the limit is taken in which the patch becomes the entire infinite tiling. “Connected” means that we subtract the contribution of spontaneous ordering, causing Bragg-like Dirac delta-function peaks to occur below the critical temperature.

The resulting $\chi(\mathbf{q})$ is a continuous function, also called the structure function giving information about the magnetic structure. It is not to be confused with

$$\mathcal{F}(\mathbf{q}) = \lim_{\mathcal{L} \rightarrow \infty} \frac{1}{\mathcal{L}} \sum_{\mathbf{r}} \sum_{\mathbf{r}'} e^{i\mathbf{q} \cdot (\mathbf{r}' - \mathbf{r})} \langle \sigma_{\mathbf{r}} \rangle \langle \sigma_{\mathbf{r}'} \rangle, \quad (32)$$

which is only nonzero below the critical temperature where $\langle \sigma_{\mathbf{r}} \rangle \equiv k'^{1/4}$. This $\mathcal{F}(\mathbf{q})$ is proportional then to the Bragg delta-function diffraction pattern that crystallographers would be most interested in.

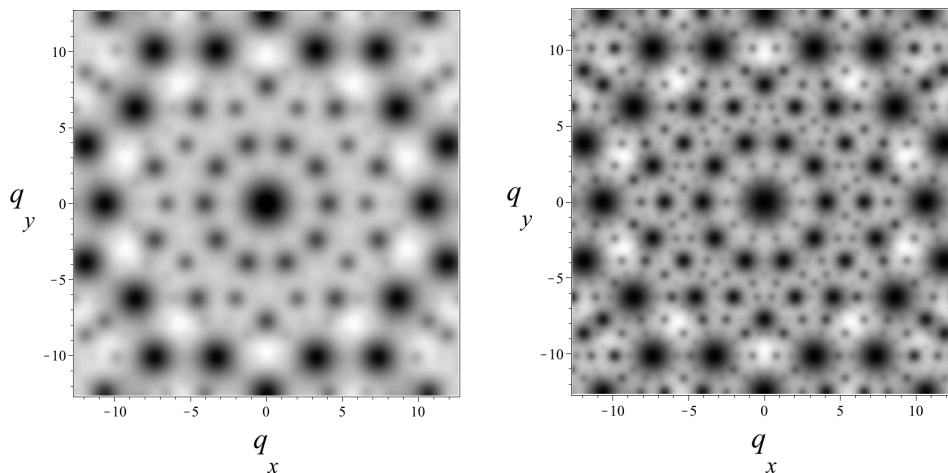


Figure 7: Density plots of $\chi(q_x, q_y)$ for $k = 0.7$. On the left: low-temperature case; on the right: high-temperature case.

The $\chi(\mathbf{q})$ can be evaluated numerically to high precision. To do this we sum first over contributions with $\mathbf{r} - \mathbf{r}'$ about the same. This is defined by taking two of the five grids of the pentagrid forming a periodic lattice with rhombus faces and taking all contributions of spins in pairs of such faces of this lattice that only differ by the same translation vector. For such a partial sum there is only little variation in the number of rapidity lines of each of the five grids passing between the spins. Finally we have to sum over all different translation vectors that give a significant contribution.

All these pieces were brought together in a long Maple program, enabling us to evaluate $\chi(\mathbf{q})$ for given \mathbf{q} to high precision [60]. As the elliptic modulus of the pentagrid Ising model approaches one, we see more and more peaks forming. In figure 7 results are shown for $k = 0.7$. Below the critical temperature part of the intensity is in Bragg peaks (Dirac delta functions) due to $\langle \sigma_i \rangle \equiv k'^{1/4} \neq 0$, which are not included in $\chi(q_x, q_y)$. There are no magnetic Bragg peaks above the critical temperature.

This explains why the $\chi(\mathbf{q})$ pattern is more intense at the same k value above the critical temperature. At the critical value of the elliptic modulus, $k = 1$, the $\chi(q_x, q_y)$ obtains everywhere dense power-law divergences, while remaining integrable over finite domains. Below criticality, the Bragg delta-function peaks of (32) are also everywhere dense, while $\mathcal{F}(\mathbf{q})$ is similarly integrable over finite domains.

7.8 Some final remarks

We note that we have also calculated $\chi(\mathbf{q})$ for Ising models on periodic lattices, but with Fibonacci-type variation of the interactions [79], which is a much easier problem. Comparison with the pentagrid Ising model results allows us to see what different effects variations of interactions or of lattice structure can have.

Finally, in this section we have shown how crucial de Bruijn's pentagrid construction is for several of the steps in the calculations within the pentagrid Ising model [60], adding some new explanations not present in our earlier work. The pentagrid picture of de Bruijn is truly powerful for calculations on Penrose tilings.

This has not always been properly understood, as a number of people have given priority to Robert Ammann for his Ammann bars, ignoring de Bruijn's work altogether. For the Penrose rhombus tiling one gets the Ammann bars by decorating the rhombi with special Ammann lines as in figure 8, providing

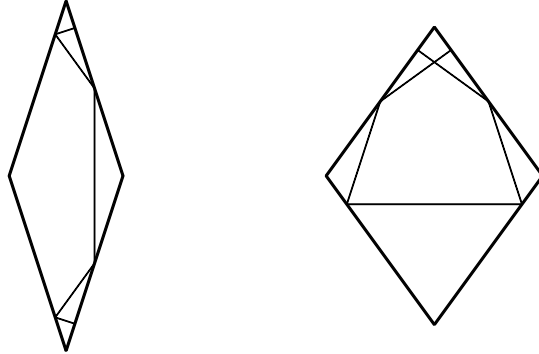


Figure 8: The skinny and fat rhombi with Ammann lines.

an alternative representation for Penrose’s matching rules. Assuming that the rhombi have sides of length 1, two sides of each rhombus are split into pieces of length $\cos(\pi/5)$ and $1 - \cos(\pi/5)$, whereas the other two sides are divided in three with lengths $1/2$, $[1 - \cos(2\pi/5)]/2$ and $\cos(2\pi/5)/2$, compare also [80].

If the rhombi are properly matched together these Ammann line pieces join to form the straight lines that are now commonly called Ammann bars, see [13, fig. 7] or [40, fig. 5]. Unlike de Bruijn’s pentagrid, the five Ammann grids are not equidistant, as the spacings now follow a Fibonacci pattern [13, 40, 81].

At this moment it is not at all clear how the work of [60] could be redone without significant extra complications using Ammann bars, even though de Bruijn has argued [33], that the Ammann quasigrd is topologically equivalent to the pentagrid. In particular, many details of [60] reviewed in subsection 7.6 depend on ratios of areas and simple translations, exploiting the grids being equidistant.

In closing, note from figure 8 that the Ammann bars intersect once on each edge of the Penrose tiling. This tempts us to propose a new Yang–Baxter integrable Ising model with Ising spins on all vertices and Ising interactions along all edges, with two especially chosen but different interactions for edges intersected by two or by three Ammann bars. Even though there seems to be no difficulty to obtain the free energy per edge in the thermodynamic limit, the determination of pair correlations cannot be done just following [65], as an odd number of rapidity lines can cross between spins, e.g. three for a neighbor pair.

Acknowledgments

This work was supported in part by the National Science Foundation under grant No. PHY-07-58139. All figures were prepared with Maple 17.

References

- [1] N.G. de Bruijn, Algebraic theory of Penrose's non-periodic tilings of the plane. I, Kon. Nederl. Akad. Wetensch. Proc. Ser. A 84 (= Indagationes Math. 43) 84 (1981) 38–52.
- [2] N.G. de Bruijn, Algebraic theory of Penrose's non-periodic tilings of the plane. II, Kon. Nederl. Akad. Wetensch. Proc. Ser. A 84 (= Indagationes Math. 43) 84 (1981) 53–66.
- [3] R. Penrose, The rôle of aesthetics in pure and applied mathematical research, Bull. Inst. Math. Appl. 10, no. 7/8 (1974) 266–271.
- [4] R. Penrose, Pentaplexity: A class of non-periodic tilings of the plane, The Mathematical Intelligencer 2 (1979) 32–37, [reprinted from Eureka 39 (1978) 16–22].
- [5] M. Gardner, Mathematical Games, Scientific American 236 #1 (1977) 110–121.
- [6] M. Gardner, Penrose Tiles to Trapdoor Ciphers ...and the Return of Dr. Matrix, W.H. Freeman and Co., New York, 1989, Revised Edition, The Mathematical Association of America, 1997, chapters 1, 2.
- [7] B. Grünbaum and G.C. Shephard, Tilings and Patterns, W.H. Freeman and Co., New York, 1987, chapter 10.
- [8] C. Kittel, Introduction to Solid State Physics, third ed., Wiley, New York, 1966.
- [9] D. Shechtman, I. Blech, D. R. Gratias, J. W. Cahn, Metallic phase with long-range orientational order and no translational symmetry, Phys. Rev. Lett. 53 (1984) 1951–1953.
- [10] D. Shechtman, I. Blech, The microstructure of rapidly solidified Al_6Mn , Metallurgical Transactions A 16 (1985) 1005–1012.

- [11] D. Levine, P.J. Steinhardt, Quasicrystals: A new class of ordered structures, *Phys. Rev. Lett.* 53 (1984) 2477–2480.
- [12] D. Levine, P.J. Steinhardt, Quasicrystals. I. Definition and structure, *Phys. Rev. B* 34 (1986) 596–616.
- [13] J.E.S. Socolar, P.J. Steinhardt, Quasicrystals. II. Unit-cell configurations, *Phys. Rev. B* 34 (1986) 617–647.
- [14] A.L. Mackay, De nive quinquangula: On the pentagonal snowflake, *Kristallografiya* 26 (1981) 910–919 [*Sov. Phys. Crystallogr.* 26 (1981) 517–522].
- [15] A.L. Mackay, Crystallography on the Penrose pattern, *Physica A* 114 (1982) 609–613.
- [16] http://www.nobelprize.org/nobel_prizes/chemistry/laureates/2011/
- [17] D. Shechtman, The discovery of quasi-periodic materials, Lecture slides, Nobel Lecture http://www.nobelprize.org/nobel_prizes/chemistry/laureates/2011/shechtman-lecture_slides.pdf
- [18] C. Kittel, *Introduction to Solid State Physics*, seventh ed., Wiley, New York, 1996.
- [19] D. Lutz, Putting quasicrystals to work, *The Industrial Physicist* 2 #4 (1996) 26, 31.
- [20] M. Jacoby, Quasicrystals: A new kind of order, *Chem. Eng. News* 77 #11 (1999) 44–47.
- [21] S. Lidin, L. Thelander, A. Fernholm, Crystals of golden proportions, http://www.nobelprize.org/nobel_prizes/chemistry/laureates/2011/popular-chemistryprize2011.pdf, p.6.
- [22] L. Guidoni, B. Dépret, A. di Stefano, P. Verkerk, Atomic diffusion in an optical quasicrystal with five-fold symmetry, *Phys. Rev. A* 60 (1999) R4233–R4236.
- [23] J. Bohannon, Quasi-crystal conundrum opens a tiling can of worms, *Science* 315 (2007) 1066.

- [24] P.J. Lu, P.J. Steinhardt, Decagonal and quasi-crystalline tilings in medieval Islamic architecture, *Science* 315 (2007) 1106–1110. See also Supporting Online Material.
- [25] R.A. Al Ajlouni, The global long-range order of quasi-periodic patterns in Islamic architecture, *Acta Cryst. A* 68 (2012) 235–243.
- [26] A. Dürer, *Underweysung der Messung, mit dem Zirckel un̄ Richtscheyt, in Linien Ebnen unnd ganzen Corporen*, Nüremberg, 1525, bk. 2, 4 figs. 24.
- [27] N.G. de Bruijn, Sequences of zeros and ones generated by special production rules, *Kon. Nederl. Akad. Wetensch. Proc. Ser. A* 84 (= *Indagationes Math.* 43) (1981) 27–37.
- [28] N.G. de Bruijn, Up-down generation of Beatty sequences. *Kon. Nederl. Akad. Wetensch. Proc. Ser. A* 92 (= *Indagationes Math.* 48) (1989) 385–407.
- [29] G.H. Hardy, E.M. Wright, *An Introduction to the Theory of Numbers*, fourth ed., Oxford University Press, London, 1960, Ch. XXIII *Kronecker's Theorem*, Theorem 445.
- [30] H. Bohr, Zur Theorie der fast periodischen Funktionen. I. Eine Verallgemeinerung der Theorie der Fourierreihen. *Acta Math.* 45 (1924) 29–127.
- [31] R. Penrose, *The Emperor's New Mind*, Penguin Books, New York, 1989, p. 344.
- [32] N.G. de Bruijn, Dualization of multigrids, *J. Phys. Colloques* 47 (1986) C3-9–C3-18.
- [33] N.G. de Bruijn, Remarks on Penrose tilings, In: *The mathematics of P. Erdős*, R.L. Graham, J. Nešetřil (eds.), vol. 2, Berlin, Springer, 1996, vol. 2, pp. 264–283.
- [34] N.G. de Bruijn, Quasicrystals and their Fourier transform, *Kon. Nederl. Akad. Wetensch. Proc. Ser. A* 89 (= *Indagationes Math.* 48) (1986) 123–152.
- [35] N.G. de Bruijn, Modulated quasicrystals. *Kon. Nederl. Akad. Wetensch. Proc. Ser. A* 90 (= *Indagationes Math.* 49) (1987) 121–132.

- [36] N.G. de Bruijn, Penrose patterns are almost entirely determined by two points, *Discrete Math.* 106/107 (1992) 97–104.
- [37] N.G. de Bruijn, Updown generation of Penrose patterns, *Indag. Mathem., N.S.*, 1 (1990) 201–220.
- [38] <http://wwwphy.princeton.edu/~steinh/> Paul Steinhardt
- [39] J.E.S. Socolar, P.J. Steinhardt, D. Levine, Quasicrystals with arbitrary orientational symmetry, *Phys. Rev. B* 32 (1985) 5547–5550.
- [40] P.J. Steinhardt, Quasicrystals: A fundamentally new phase of solid matter exhibits symmetries that are impossible for ordinary crystals, *American Scientist* 74 (1986) 586–597.
- [41] L. Bindi, P.J. Steinhardt, N. Yao, P.J. Lu, Natural Quasicrystals, *Science* 324 (2009) 1306–1309.
- [42] P.J. Steinhardt and L. Bindi, Once upon a time in Kamchatka: The search for natural quasicrystals, *Phil. Mag.* 91 (2011) 2421–2426.
- [43] L. Bindi, P.J. Steinhardt, N. Yao, P.J. Lu, Icosahedrite, $\text{Al}_{63}\text{Cu}_{24}\text{Fe}_{13}$, the first natural quasicrystal, *American Mineralogist* 96 (2011) 928–931.
- [44] H. Tsunetsugu, T. Fujiwara, K. Ueda, T. Tokihiro, Electronic properties of the Penrose lattice. I. Energy spectrum and wave functions, *Phys. Rev. B* 43 (1991) 8879–8891.
- [45] M. Baake, U. Grimm, R.V. Moody, Die verborgene Ordnung der Quasikristalle, *Spektrum der Wissenschaft*, Heft 02 (Februar 2002) 64–74, [in German, English translation: What is Aperiodic Order?, arXiv:math.HO/0203252].
- [46] The Tilings Encyclopedia, <http://tilings.math.uni-bielefeld.de>.
- [47] P. Gummelt, Penrose tilings as coverings of congruent decagons, *Geometriae Dedicata* 62 (1996) 1–17.
- [48] P.J. Steinhardt, H.C. Jeong, A simpler approach to Penrose tilings with implications for quasicrystal formation, *Nature* 382 (1996) 431–433.

- [49] H.-C. Jeong, P.J. Steinhardt, Constructing Penrose-like tilings from a single prototile and the implications for quasicrystals, *Phys. Rev. B* 55 (1997) 3520–3532.
- [50] P.J. Steinhardt, H.-C. Jeong, K. Saitoheong, M. Tanaka, E. Abe, A.P. Tsai, Experimental verification of the quasi-unit-cell model of quasicrystal structure *Nature* 396 (1998) 55–57, 399 (1999) 84.
- [51] P.J. Steinhardt, Penrose tilings, cluster models and the quasi-unit cell picture, *Mater. Sci. Eng. A* 294–296 (2000) 205–210.
- [52] E.A. Lord, S. Ranganathan, The Gummelt decagon as a ‘quasi unit cell’, *Acta Cryst. A* 57 (2001) 531–539.
- [53] H.C. Jeong, P.J. Steinhardt, Rules for computing symmetry, density, and stoichiometry in a quasi-unit-cell model of quasicrystals, *Phys. Rev. B* 68 (2003) 064102 (9 pp.).
- [54] E. Abe, K. Saitoh, H. Takakura, A.P. Tsai, P.J. Steinhardt, H.-C. Jeong, Quasi-Unit-Cell Model for an Al-Ni-Co Ideal Quasicrystal based on Clusters with Broken Tenfold Symmetry, *Phys. Rev. Lett.* 84 (2000) 4609–4612.
- [55] P. Gummelt, C. Bandt, A cluster approach to random Penrose tilings, *Mater. Sci. Eng. A* 294–296 (2000) 250–253.
- [56] F. Gähler, M. Reichert, Cluster models of decagonal tilings and quasicrystals *J. Alloys Compd.* 342 (2002) 180–185.
- [57] M. Reichert, F. Gähler, Cluster model of decagonal tilings, *Phys. Rev. B* 68 (2003) 214202 (10 pp.).
- [58] H. Au-Yang, J.H.H. Perk, Overlapping unit cells in 3d quasicrystal structure, *J. Phys. A: Math. Gen.* 39 (2006) 9035–9044. (See also arXiv:cond-mat/0507117.)
- [59] H. Au-Yang, J.H.H. Perk, Quasicrystals: Projections of 5-d lattice into 2 and 3 dimensions, in: M.-L. Ge, W. Zhang (Eds.), *Differential Geometry and Physics*, Nankai Tracts in Mathematics, Vol. 10, World Scientific, Singapore, 2006, pp. 123–132. (See also arXiv:math-ph/0606028.)

- [60] H. Au-Yang, J.H.H. Perk, Q -dependent susceptibilities in Z -invariant pentagrid Ising models, *J. Stat. Phys.* 127 (2007) 221–264. (See also arXiv:cond-mat/0409557.)
- [61] H.S. Green and C.A. Hurst, *Order-Disorder Phenomena*, Interscience Publ., Wiley & Sons, London, 1964.
- [62] B.M. McCoy and T.T. Wu, *The Two-Dimensional Ising Model*, Harvard Univ. Press, Cambridge, Mass., 1973.
- [63] J.H.H. Perk, H. Au-Yang, Yang–Baxter Equation, in: J.-P. Francoise, G.L. Naber, Tsou S.T. (Eds.), *Encyclopedia of Mathematical Physics*, eds. J.-P. Francoise, G.L. Naber and Tsou S.T., Vol. 5, Oxford: Elsevier Science, 2006, pp. 465–473. (Extended version in arXiv:math-ph/0606053.)
- [64] C.N. Yang, The spontaneous magnetization of a two-dimensional Ising model, *Phys. Rev.* 85 (1952) 808–816.
- [65] R.J. Baxter, Solvable eight vertex model on an arbitrary planar lattice, *Phil. Trans. R. Soc. Lond. A* 289 (1978) 315–346.
- [66] V.E. Korepin, Eight-vertex model of the quasicrystal, *Phys. Lett. A* 118 (1986) 285–286.
- [67] V.E. Korepin, Completely integrable models in quasicrystals, *Commun. Math. Phys.* 110 (1987) 157–171.
- [68] N.V. Antonov and V.E. Korepin, Critical properties and correlation functions of the eight-vertex model on a quasicrystal, *Zap. Nauch. Semin. LOMI* 161 (1987) 13–23 [*J. Sov. Math.* 46 (1989) 2058–2065].
- [69] N.V. Antonov and V.E. Korepin, Critical properties of completely integrable spin models in quasicrystals, *Teor. Mat. Fiz.* 77 (1988) 402–411 [*Theor. Math. Phys.* 77 (1988) 1282–1288].
- [70] R.J. Baxter, *Exactly Solved Models in Statistical Mechanics*, Academic Press, London, 1982.
- [71] H. Au-Yang and J.H.H. Perk, Critical correlations in a Z -invariant inhomogeneous Ising model, *Physica A* 144 (1987) 44–104.

- [72] T.C. Choy, Ising models on two-dimensional quasi-crystals: Some exact results, *Intern. J. Modern Phys. B* 2 (1988) 49–63.
- [73] J.H.H. Perk, Quadratic identities for Ising model correlations, *Phys. Lett. A* 79 (1980) 3–5.
- [74] J.H.H. Perk, H.W. Capel, G.R.W. Quispel and F.W. Nijhoff, Finite-temperature correlations for the Ising chain in a transverse field, *Physica A* 123 (1984) 1–49.
- [75] H. Au-Yang and J.H.H. Perk, Wavevector-Dependent Susceptibility in Aperiodic Planar Ising Models, in: *MathPhys Odyssey 2001: Integrable Models and Beyond*, M. Kashiwara and T. Miwa, eds., (Birkhäuser, Boston, 2002), pp. 1–21.
- [76] H. Au-Yang and J.H.H. Perk, Correlation Functions and Susceptibility in the Z -Invariant Ising Model, in: *MathPhys Odyssey 2001: Integrable Models and Beyond*, M. Kashiwara and T. Miwa, eds., (Birkhäuser, Boston, 2002), pp. 23–48.
- [77] N.S. Witte, Isomonodromic deformation theory and the next-to-diagonal correlations of the anisotropic square lattice Ising model, *J. Phys. A: Math. Theor.* 40 (2007) F491–F501 (2007). See also arXiv:0705.0557.)
- [78] Y. Chan, A.J. Guttmann, B.G. Nickel and J.H.H. Perk, The Ising Susceptibility Scaling Function, *J. Stat. Phys.* 145 (2011) 549–590. (See also arXiv:1012.5272.)
- [79] H. Au-Yang, J.H.H. Perk, Q -dependent susceptibilities in ferromagnetic quasiperiodic Z -invariant Ising models, *J. Stat. Phys.* 127 (2007) 265–286. (See also arXiv:cond-mat/0606301.)
- [80] T. Stehling, Ammann bars and quasicrystals, *Discrete Comput. Geom.* 7 (1992) 125–133.
- [81] R. Lück, Basic ideas of Ammann bar grids, *Intern. J. Mod. Phys. B* 7 (1993) 1437–1453.